Journal of Asian Scientific Research

journal homepage:http://www.aessweb.com/journals/5003

THEORETICAL TREATMENT OF KRYPTON ION BEAM BOMBARDEMENT IN ZINC TARGET

A.M. Abdelraheem

Accelerators & Ion Sources Department, Nuclear Research Center, Atomic Energy Authority, Inchas, Cairo, Egypt

M.M. Abdelrahman

Accelerators & Ion Sources Department, Nuclear Research Center, Atomic Energy Authority, Inchas, Cairo, Egypt

H. El-Khabeary

Accelerators & Ion Sources Department, Nuclear Research Center, Atomic Energy Authority, Inchas,, Cairo, Egypt

ABSTRACT

The manuscript reports a study of Kr ion implantation in a Zn target in the 10-50 keV energy range at different source parameters, which combines experimental data and simulation with the SRIM package. The implanted thickness for the 45 keV was found to be 10 µm. The ion penetration depths for different films at different energies (10-50 keV) were calculated using SRIM computer program and found to be 100 Å at 10 keV and 475 Å at 40 keV. Theoretical calculations using SRIM-2000 have been performed to investigate the ion range. The dependence of ion beam currents on the accelerating voltage is given at discharge current equal to 0.8A and for various pressures. The krypton ion beam current reaches 3mA at 45KV for a pressure of 2 x 10-5Torr and a cathode current equal to 130A. An analysis has been made for an implanted krypton ion beam in a zinc specimen using laser ablation inductively coupled plasma mass spectrometry. Photographs show the examined zinc specimens are presented. The depth profile shows that the highest concentration of krypton ions under the surface of the zinc specimen is located at about 10 µm.

© 2014 AESS Publications. All Rights Reserved.

Keywords: Freeman ion source, Krypton ion beam applications, SRIM program.

1. INTRODUCTION

The ion source is the beginning of the ion process, whatever the application is to be. The ion beam is created at the source, transport over distances from a meter or so up to many hundreds of meters and delivered to the intended device or use. The physics and technology of beam transport [1, 2] is a sibling field to that of ion sources which attains increasing importance as the required

beam transport efficiency and the beam current density increase. Understanding of the physical principles of ion source design and operation has increased greatly in recent years and the technology of their construction and application has similarly flourished. Fields of use both in fundamental science and in applied technology call for increasing formidable ion beam parameters and sophisticated ion source performance. Stopping and Range of Ions in Matter (SRIM) is a group of computer programs which calculate interaction of ions with matter; the core of SRIM is a program Transport of ions in matter (TRIM). The programs were developed by James *et al.* [3] and are being continuously upgraded with the major changes occurring approximately every five years. SRIM is based on a Monte Carlo simulation method, namely the binary collision approximation with a random selection of the impact parameter of the next colliding ion. As the input parameters, it needs the ion type and energy (in the range 10 eV – 2 GeV) and the material of one or several target layers.

The programs are made so they can be interrupted at any time, and then resumed later. They have a very easy-to-use user interface and built-in default parameters for all ions and materials. Those features made SRIM immensely popular. However, it doesn't take account of the crystal structure nor dynamic composition changes in the material that severely limits its usefulness in some cases.

The Freeman ion source is still the most versatile and most widely used ion source. Its ability to produce sharply focused milliampere beams of most elements over a wide range of energies continues to make it a popular choice of ion source. For use in semiconductor ion implanters its performance and relative ease of operation has led to it being extensively used for the production doping of silicon devices. Freeman sources [4, 5] are used extensively in the semiconductor ion implantation field. A high current heavy ion source system of Freeman type has been installed [6] at the Accelerators and Ion Sources Department, Nuclear Research Center, A.E.A., Egypt. This source [7] is supplied by Efremov Research Institute of Electrophysical Apparatus, Saint Petersburg, Russia. The extracted ion beams are particularly quiescent and stable and we used before [8] different elements such as Sb, $Ticl_3$, KI and Bi. The intended applications at the department are ion beam lithography, micro machining, material surface characterization using finely focused beams and further to be used for isotope separation. Most aspects of the energy loss of ions in matter [9,10] are calculated in SRIM, includes quick calculations which produce tables of stopping powers, range and straggling distributions for any ion at any energy in any elemental target. More elaborate calculations include targets with complex multi-layer configurations. In this work, a study and investigation of Kr ion implantation in a Zn target in the 10-50 keV energy range at different gas pressures, which combines experimental data and simulation with the SRIM package, were done. Experimentally, the implanted thickness for the 45 keV was found to be 10 μm. Theoretically, the ion penetration depths for different films at different energies (10-50 keV) were calculated using SRIM computer program and found to be 100 Å at 10 keV and 475 Å at 40 keV.

1.1. Description of the Ion Source

Ions of various elements are generated in a Freeman type ion source and accelerated in a four electrode acceleration / deceleration system to obtain energy of up to 50 KeV. The ion source and

the accelerating system are constructed as a single cement unit mounted on the vacuum chamber of the system. For measuring the ion beam current at the outlet aperture, a movable Faraday cup is installed in the vacuum chamber. The vacuum system comprises two turbomolecular pumps, each with a pumping rate of 950 L/S mounted on the chamber via vacuum gate valves and fore vacuum pumping station.

The Freeman ion source and the acceleration system are shown in Fig 1. It consists of a thermoemission tungsten cathode rod with 2mm diameter, fixed inside a molybdenum anode by boron nitride insulators. The anode has an emission slit 40 mm in length and 0.5 – 2 mm wide, which is formed by two replaceable molybdenum plates mounted between the anode and the emission electrode, where the distance between the cathode and the exit slit is equal to 3.7 mm. An auxiliary magnetic field of 100 gauss is maintained parallel to the axis of the cathode. The anode contains three holes for feeding with gas, liquid or solid materials.

Fig-1. The schematic diagram of the Freeman ion source system.

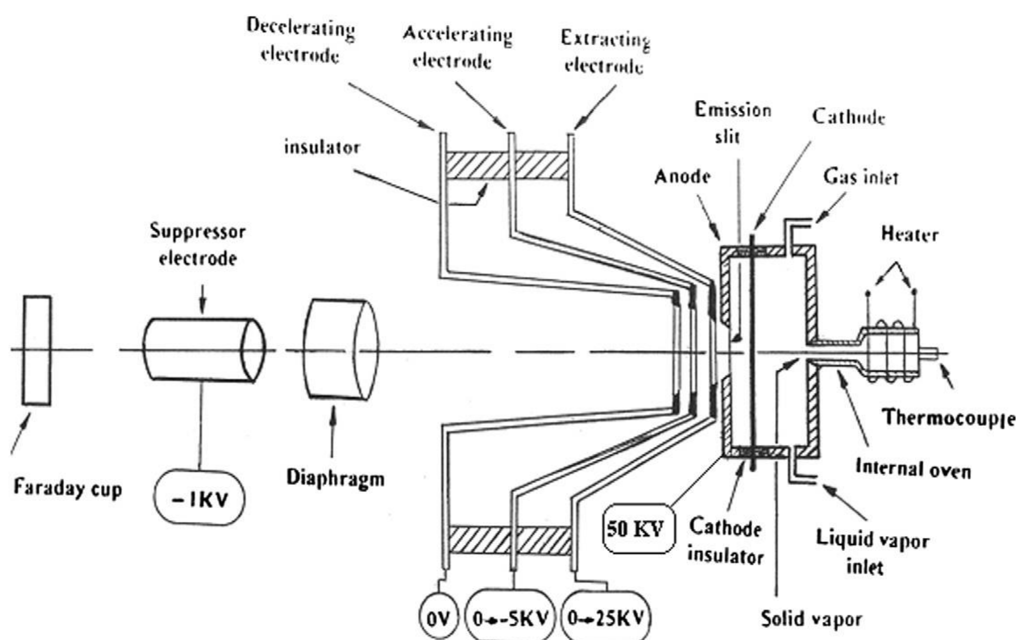

1.2. Theoretical Treatment

The simulation was made using SRIM 3D computer program. The simulation studied the ions distribution and recoil distribution of Krypton ion beam on zinc target with different energies. The actual integrated distance traveled by the ion is called the range. The ion's net penetration into the material, measured along the vector of the ion's incident trajectory, which is perpendicular to the surface in this example, is called the projected range.

The stopping power due to electronic stopping is proportional to the charge of the ion. Therefore the projected range decreases with increasing ion charge. In principle the stopping power due to nuclear stopping also increases with increasing ion charge, but the nuclear stopping power reaches a maximum at certain energy and this maximum moves to higher energies if the ion charge is increased. For low ion energies the stopping power can therefore be inversely proportional to the charge of the ion**.**

Figs.2, 3, 4, 5 and 6 show the ions distribution on the zinc target surface at different ion energies equal to 10, 20, 30, 40 and 50 keV using krypton gas.

Fig-2. Krypton ion distribution on zinc target energy equal to 10 keV

Ion Distribution

Ion Range = 57 A Skewness = 0.623
Straggle = 28 A Kurtosis = 3.387

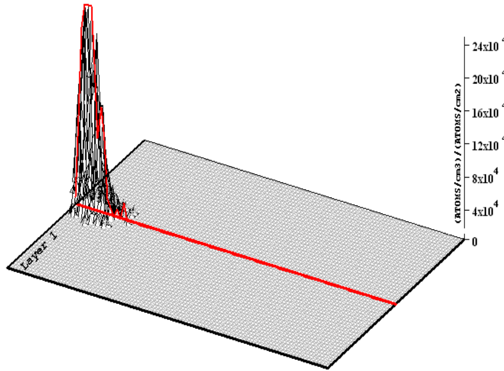

Plot Window goes from 0 A to 1000 A; cell width = 10 A
Press PAUSE TRIM to speed plots. Rotate plot with Mouse.

Ion = Kr (10. keV)

Fig-3. Krypton ion distribution on zinc targetat at energy equal to 20 keV

Ion Distribution

Ion Range = 88 A Skewness = 0.574
Straggle = 44 A Kurtosis = 3.228

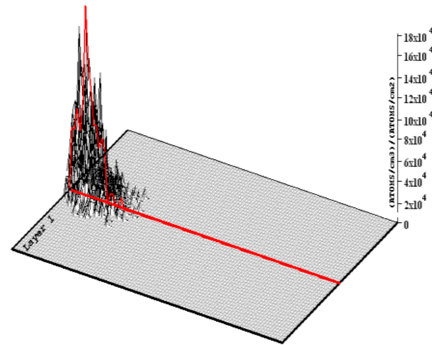

Plot Window goes from 0 A to 1000 A; cell width = 10 A
Press PAUSE TRIM to speed plots. Rotate plot with Mouse.

Ion = Kr (20. keV)

Fig-4. Krypton ion distribution on zinc target at energy equal to 30 keV

Ion Distribution

Ion Range = 117 A Skewness = 0.623
Straggle = 60 A Kurtosis = 3.002

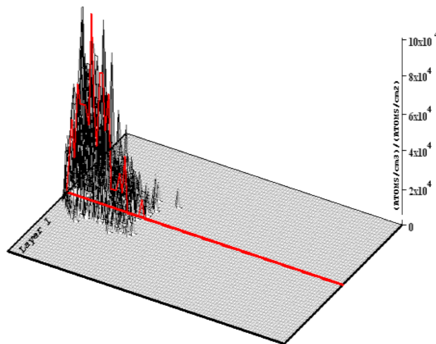

Plot Window goes from 0 A to 1000 A; cell width = 10 A
Press PAUSE TRIM to speed plots. Rotate plot with Mouse.

Ion = Kr (30. keV)

Fig-5. Krypton ion distribution on zinc target at at energy equal to 40 keV

Ion Distribution

Ion Range = 148 A Skewness = 0.566
Straggle = 73 A Kurtosis = 3.034

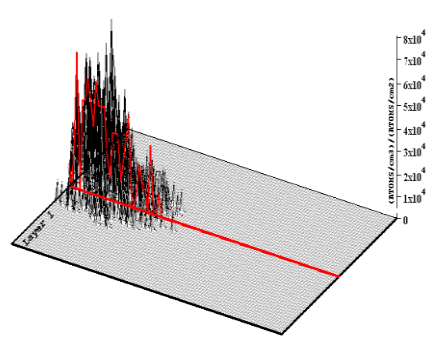

Plot Window goes from 0 A to 1000 A; cell width = 10 A
Press PAUSE TRIM to speed plots. Rotate plot with Mouse.

Ion = Kr (40. keV)

Fig-6. Krypton ion distribution on zinc target at energy equal to 50 keV at different energies.

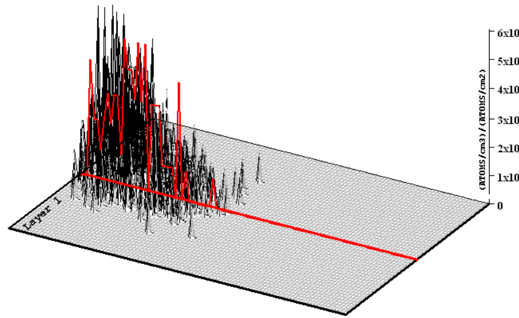

Fig-7. Krypton ion stoppping range in zinc target at different energies.

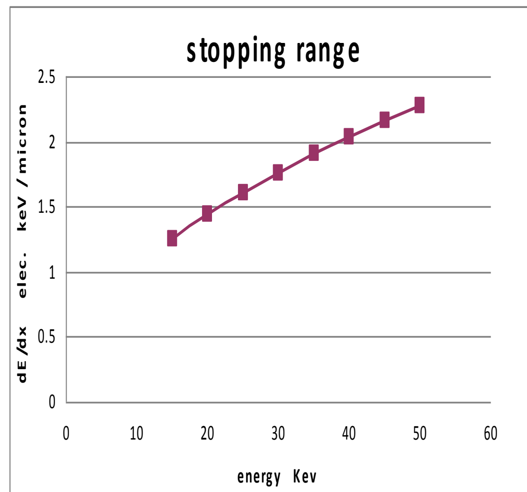

Fig.7 shows Krypton ion stoppping range in zinc target at different energies. It is clear that Krypton ion stoppping range in zinc target increases with increasing ion energy.

Fig.8 shows the energy loss of Krypton ions in zinc target for ionization, vacancies and photons using different ion energy. It is clear that at constant ion energy, the energy loss of Krypton ions in zinc target for ionization is higher than that for vacinces and photons.

Fig.9 shows Krypton ions range in zinc target at different energies. It is obvious that the ions range increases with increasing ions energy, but the ions range in case of longitudenal is higher than that in case of lateral project and radial.

Fig-8. Krypton ion energy loss in zinc target at different energies.

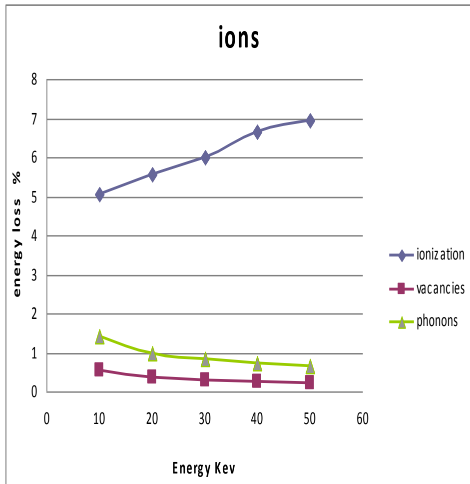

Fig-9. Krypton ion range in zinc target at different energies.

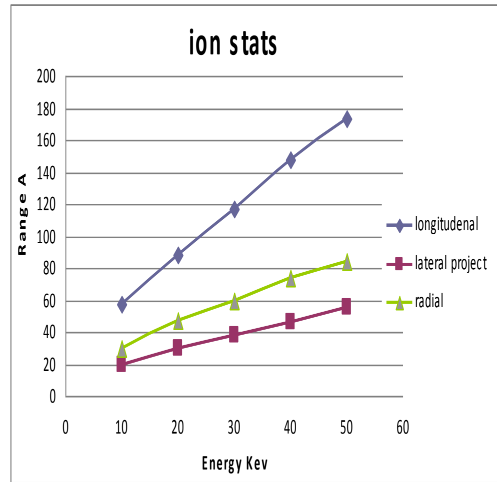

Fig.10 shows krypton ions sputtering yield of zinc target at different ions energy. It is obvious that the sputtering yield increases with increasing krypton ions energy and the sputtering yield in case of (eV / atoms) is higher than in case of (atoms / ions).

Fig-10. Krypton ion sputtering yield at different energies using zinc target.

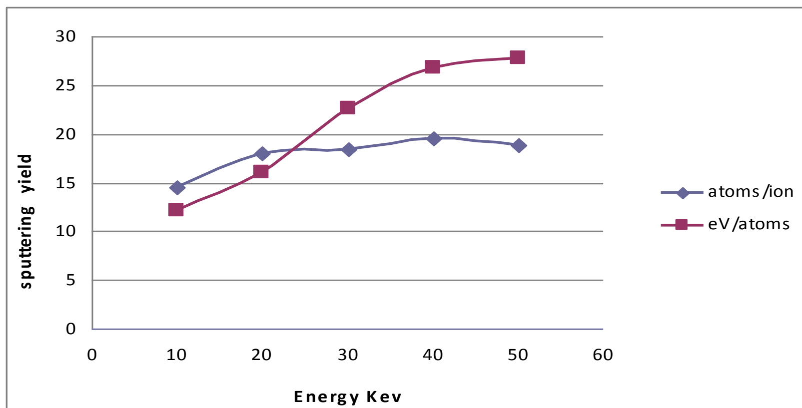

Figs 11,12 show the depth penetration for krypton ions in zinc target at two energies 10, 40 keV, respectively. The depth penetration at those two energies was found to be 100 **Å** , 475 **Å** , respectively. where, at lower energy, the depth penetration was lower than at higher energy(40keV).

Fig-11. Depth penetration for kryption ions in zinc target at 10 keV.

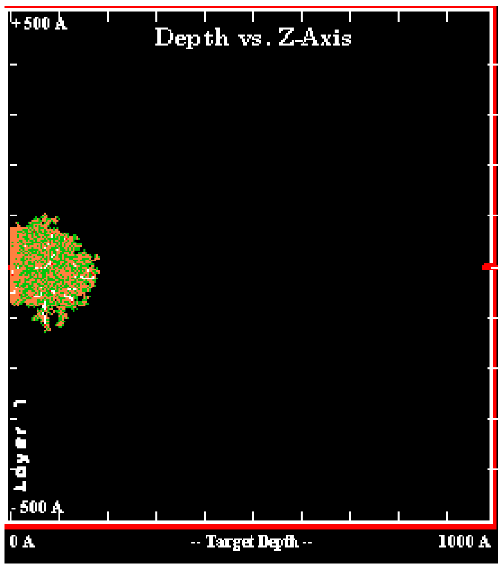

Fig. 12.Depth penetration for kryption Ions in zinc target at 40 keV.

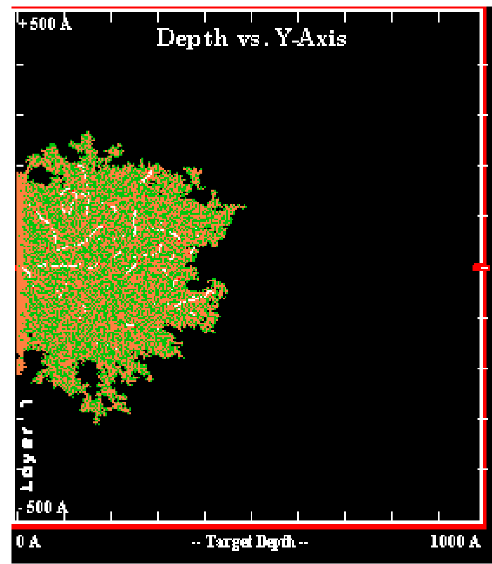

1.3. Applications of Krypton Ion Beam

The movable Faraday cup is designed for measuring a total beam current at the source outlet, for shutoff a beam to control the exposure time. The Faraday cup is mounted in the vacuum chamber. The zinc specimen was placed at a distance of 1cm from the Faraday cup. This specimen has a thickness of 1.5 mm and has been exposed to the krypton ion beam for a period of 3 hours.

The operating parameters for the ion source were kept as follows: V_{acc} = 40KV, V_{ex}= 17 KV, I_{ex}= 0.6 mA, I_b= 7.2mA, I_d =1A, V_d = 61V and at a pressure of $3x10^{-5}$ Torr [11].

The zinc specimen was examined using laser ablation inductively coupled plasma mass spectrometry [12] (LA-ICP-MS). Fig.13 shows the surface of the polished zinc specimen before exposure to the krypton ion beam. Fig.14 shows the surface of the zinc specimen after exposure to the krypton ion beam without laser ablation (without any shots). Fig.15 shows the zinc specimen exposed to the krypton ion beam after ablation by laser.

Fig-13. Zinc surface picture before exposure to krypton ion beam**.**

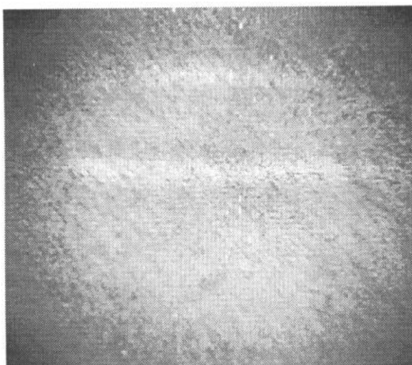

Fig-14. Zinc surface picture after exposure to krypton ion beam**.**

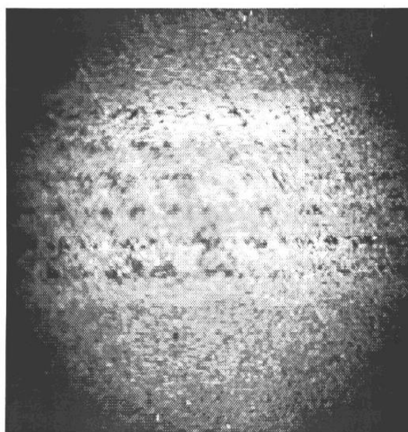

Fig-15. Zinc target surface picture exposed to krypton ions after ablation by laser.

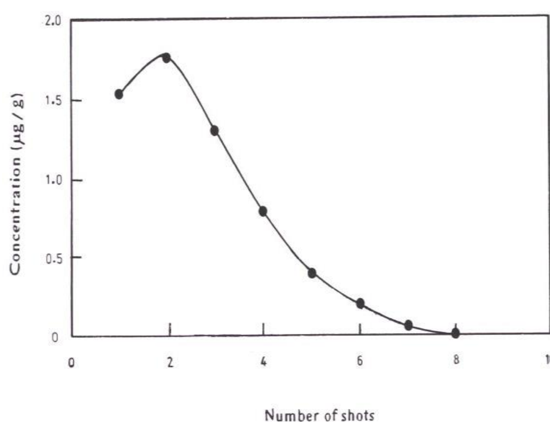

Fig-16. Depth distribution of krypton ions into Zinc target surface.

Fig.16 shows the depth distribution of krypton ions in the surface of the zinc specimen after implantation by krypton ion beam. The depth profile [13] shows that the highest concentration of krypton ions under the surface of the zinc specimen is located at about 10 μm. The profile shows a tail in the low concentration region, which is attributed due to fragmentation and energy contamination.

2. CONCLUSION

The experimental study yielded a practical method of adjusting the different source parameters added with a theoretical analysis using a SRIM program was done for a Kr ion implantation produced from Freeman type ion source in a Zn target in the 0-50 keV energy range**.** The implanted thickness for the 45 keV was found to be 10 μm. The ion penetration depths for different films at different energies (10-50 keV) were calculated using SRIM computer program and found to be 100Å at 10 keV and 475 Å at 40 keV. The depth profile shows that the highest concentration of krypton ions under the surface of the zinc specimen is located at about 10 μm. The exact knowledge of these parameters is necessary in order to plan correctly for implantation using ion beams with energies in the kilovolts range. Applications such as ion beam lithography and materials surface characterization using ion beams call for relatively low current, finely focused beams with high efficiency and the excellent performance of this ion source made it successful for these purposes.

REFERENCES

[1] D. Aitken, *The physics and technology of ion sources*. New York: John Wiley and Sons, 2004.

[2] M. C. Bradage and A. Gleizes, "Phenomena in ionized gases," *xxx Int. Conf.,* vol. 4, p. 42, 1997.

[3] F. Z. James, P. B. Jochen, and D. Z. Matthias, *SRIM - The stopping and range of ions in matter*. North Carolina, USA: Lulu Press Co., 2008.

[4] G. Christoph, *Lecture series"Ion sources & Diagnostics"*. ASTeC (south): Rutherford Appleton Laboratory RAL, Accelerator Science & Technology Centre, 2011.

[5] S. Nikiforov, V. Golubev, D. Solnyshkov, and M. Svinin, "Proceeding of EPAC95," Dallas, USA, 1995.

[6] F. W. Abdel Salam, A. G. Helal, A. A. Ghanem, K. M. Khalefa, and Al-Azhar, "Eng. Fifth Int. Conf., Dec," 1997.

[7] M. M. Abdelrahman and F. W. Abdelsalam, *Nuclear Instruments and Methods in Physics Research B* vol. 269 pp. 1761–1766, 2011.

[8] F. W. Abdel Salam, A. G. Helal, A. A. Ghanem, and N. T. EL-Merai, "The 3rd Int. Conf.on Eng. Math. and Phys," Cairo Univ, 1997.

[9] M. Nastasi and J. W. Mayer, *Ion implantation and synthesis of materials*. New York: Springer Berlin Heidelberg, 2006.

[10] J. Norem, Z. Insepov, and I. Konkashbaev, *Nucl. Instrum. Meth. Phys. Res. Sec. A,* vol. 537, p. 510, 2005.

[11] F. W. Abdel Salam, A. G. Helal, H. El-Khabeary, M. M. Abdel Rahman, and K. M. Khalefa, "Production and diagnosis of krypton ion beam using a Freeman ion source," in *Proc.of the 3rd conf. on Nuclear and Particle Physics (NUPPAC' 01)*, Cairo, Egypt, 2001, pp. 20-24.

[12] N. F. Zahran, M. A. Amr, A. A. Youssef, and A. I. Helal, "Fifth Radiation Phys. Conf," Cairo, Egypt, 2000, p. 273.

[13] J. S. Becker and H. J. Dietze, *Inter.J.*mass *Spectrom,* vol. 197, p. 1, 2000.